

far applied the technique only to single crystals. It should be applicable to powder samples as well.

We wish to thank Dr. H. Alperin for helpful comments on the manuscript.

¹R. M. Bozorth, V. Kramer, and J. P. Remeika, *Phys. Rev. Letters* **1**, 3 (1958).

²E. M. Gyorgy, J. P. Remeika, and F. B. Hegedorn, *J. Appl. Phys.* **39**, 1369 (1968).

³G. Gorodetsky and L. M. Levinson, *Solid State Commun.* **7**, 67 (1969).

⁴G. Gorodetsky, L. M. Levinson, S. Shtrikman, D. Treves, and B. M. Wanklyn, *Phys. Rev.* **187**, 637 (1969).

⁵R. W. Grant and S. Geller, *Solid State Commun.* **7**, 1291 (1969).

⁶G. E. Bacon, *Neutron Diffraction* (Oxford U. P., Oxford, England, 1962), p. 163.

⁷S. Geller, *J. Chem. Phys.* **24**, 1236 (1956).

⁸V. W. Arndt and B. T. M. Willis, *Single Crystal Diffractometry* (Cambridge U. P., Cambridge, England, 1968), p. 247.

PHYSICAL REVIEW B

VOLUME 3, NUMBER 11

1 JUNE 1971

Magnetoresistance Measurements on Ferromagnetic PdFe and PdCo Alloys*

Gwyn Williams

*Department of Physics, University of Manitoba, Winnipeg, Canada and
School of Mathematical and Physical Sciences, University of Sussex,
Brighton, Sussex, United Kingdom*

and

G. A. Swallow and J. W. Loram

*School of Mathematical and Physical Sciences, University of Sussex,
Brighton, Sussex, United Kingdom*

(Received 27 January 1971)

The temperature dependence of the resistivity of a Pd-0.78-at.% Fe alloy and a Pd-0.73-at.% Co alloy has been measured in the temperature region 1.4–20 K, and in applied fields up to 60 kOe. These data can be fitted simply by including the effects of the applied field in a model due to Long and Turner; this model, based on *s*-electron scattering from collective excitations in the coupled impurity-moment *d*-band system of the alloy, satisfactorily accounts for the majority of the zero-field properties of this class of alloy. Analysis of the PdFe data yields $g=2$, while the acoustic spin-wave stiffness *D* is found to be field dependent. Various origins of this field dependence are discussed. For the PdCo system this scheme of analysis requires the splitting factor *g* to be significantly less than 2. The *D* is again found to be field dependent.

I. INTRODUCTION

The properties of alloys of Pd with the transition metals Fe and Co exhibit many anomalous features, of which (i) the giant moment phenomenon¹⁻⁴ and (ii) the rapidly increasing magnetic-ordering temperature T_c with relatively low impurity concentration⁵ *c* have received the most experimental and theoretical attention. The origin of both (i) and (ii) lies in the nearly ferromagnetic, itinerant character of the Pd *d* band. The conventional Ruderman-Kittel-Kasuya-Yosida (RKKY) oscillations⁶ induced in the host conduction band via an exchange coupling of the form $-2J\vec{S}\cdot\vec{\sigma}$ between the impurity spin (\vec{S}) and the conduction-electron spin ($\vec{\sigma}$) are, in this case,⁷ suppressed to relatively large distances by the effects of exchange enhancement.^{8,9} Consequently, there is an enhancement in the *range* of the induced polarization, as evidenced by neutron diffraction¹⁰ and Mössbauer data.^{11,12}

Clogston *et al.*³ used the concept of a magnetized virtual bound state to discuss the static magnetic properties of these alloys, while Rhodes and Wohlfarth¹³ have used a rigid-band model in their theoretical discussion. More recently Moriya¹⁴ has given careful consideration to these static properties on the basis of the Anderson model.¹⁵

The dynamic properties of these alloys in the ferromagnetic state were first investigated by Doniach and Wohlfarth¹⁶; this work was later extended by Cole and Turner,¹⁷ who concluded that the dynamical spin states could, at temperatures well below the magnetic-ordering temperature T_c be approximately described by spin waves. In a recent publication by Long and Turner¹⁸ the resistivity of this class of alloy has been calculated on the basis of this dynamical model; the conductivity is regarded as being dominated by *s* electrons (in view of their relatively low effective mass^{19,20}) which scatter from the collective excitations in two

ways: first, by scattering from the impurity spin system via "direct" exchange coupling at impurity sites, and second, via the excitation of an electron-hole pair in the coupled d band of the alloy, which subsequently scatters from an impurity spin. Since the spin system is not translationally invariant, momentum is not conserved during a scattering event. This leads at low temperatures ($T \ll T_c$) to an incremental resistivity $\Delta\rho(T) [= \rho_{\text{alloy}}(T) - \rho_{\text{Pd}}(T)]$ which has a $T^{3/2}$ limiting temperature dependence. The inclusion of the effects of an applied magnetic field in this type of calculation is quite straightforward.²¹

In this paper we present magnetoresistance measurements in the temperature range 1.4–20 K, and in magnetic fields up to 60 kOe, on a Pd-0.78-at. % Fe alloy and a Pd-0.73-at. % Co alloy. An analysis of the data in terms of the above model is presented. These alloys were chosen since the range of validity of the equations used to fit the magnetoresistance measurements was expected—for alloys of this concentration—to extend to around 12 K. For alloys of higher concentration the expected range of validity extends to higher temperatures, but above about 12 K the situation is complicated by the breakdown of Matthiessen's rule²² due to the presence of several different scattering mechanisms with different anisotropies²³ (in this case phonon and magnon scattering). In addition, for more concentrated alloys the temperature variation of the resistivity (and hence the change of resistivity in an applied field) is less rapid; these alloys thus represent an optimization of these two aspects.

II. EXPERIMENTAL DETAILS

The alloys examined were taken from those previously studied in zero magnetic field down to 0.45 K.^{24,25} The samples were prepared from 99.999%-pure Pd and 99.999%-pure Fe (both supplied by Johnson Matthey and Co., London) or 99.99%-pure Co (from Koch-Light Ltd., England) by a previously described method.²⁵ The magnetoresistance samples in the form of carefully etched and annealed strips, approximately 0.01 cm thick, 0.2 cm wide, and 8 cm long, were mounted in the longitudinal field of a 60-kOe superconducting solenoid. During the course of the measurements the solenoid was locked in its persistent mode; the applied magnetic field, measured to within ± 0.1 kOe using a Hall probe, varied by approximately 2 parts in 10^3 over the length of the sample. The solenoid itself was immersed in a He⁴ bath maintained at 4.2 K; the magnetoresistance sample was mounted in an enclosure which could be inserted into the bore of the solenoid and which, in addition, could be thermally isolated from the main He⁴ bath. Temperature stabilization of this enclosure was accomplished using a carbon resistance thermometer (100- Ω

Speer) in a feedback control circuit, the output from which was fed into heaters wound around the insert. In this way temperatures below 4.2 K were stabilized and measured to ± 1 millidegree (by observing the He⁴ vapor pressure), and temperatures above 4.2 K were stabilized and measured to better than $\pm 1\%$ (using gas-thermometer techniques). The sample resistances were measured using a four-probe technique in which the sample current was altered to balance a highly stable voltage. Reproducible measurements to $\pm 10^{-9}$ V were achieved by measuring the sample voltage and current with Hewlett-Packard digital voltmeters; a Keithley 149 millimicrovoltmeter was used to detect the balanced condition. The estimated accuracy of the resistance measurement is 1 part in 10^4 . Reliable estimates of the incremental resistivity of the alloy were made by measuring the area-to-length ratio of the samples to within $\pm 0.5\%$, using a method described by Loram, Whall, and Ford.²⁶

III. RESULTS AND DISCUSSION

In order to facilitate analysis of the experimental data, the sample resistances were measured in constant magnetic fields (of approximate magnitude 10, 25, and 59 kOe) as a function of temperature in the interval 1.4–20 K. In order to estimate the incremental resistivity of the alloy $\Delta\rho(T) [= \rho_{\text{alloy}}(T) - \rho_{\text{Pd}}(T)]$ it was necessary to measure the resistivity of a pure-Pd sample.

A. Pure-Pd Resistivity

In Fig. 1 the measured resistivity of the Pd sample $\rho_{\text{Pd}}(T)$ is plotted as a function of temperature T up to about 10 K; in Fig. 2, $\rho_{\text{Pd}}(T)$ is plotted against T^2 . This figure indicated that up to about 6 K the resistivity of the pure metal is well represented by

$$\rho_{\text{Pd}}(T) = \rho_0 + AT^2, \quad (1)$$

with ρ_0 estimated at $8.98 \times 10^{-2} \mu\Omega \text{ cm}$, and A is approximately $29 \times 10^{-6} \mu\Omega \text{ cm/K}^2$. The functional

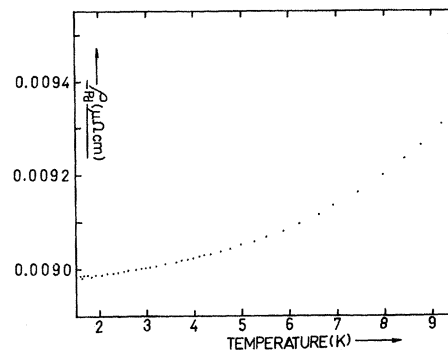


FIG. 1. The resistivity of the Pd sample $\rho_{\text{Pd}}(T)$ ($\mu\Omega \text{ cm}$) plotted against temperature (K).

form for $\rho_{Pd}(T)$ given in Eq. (1) agrees with previous measurements on Pd by Schindler and Rice²⁷ over a comparable temperature range; these authors estimate A to be $26 \times 10^{-6} \mu\Omega \text{ cm}/\text{K}^2$. This T^2 contribution to the resistivity is believed to originate from s electrons scattering from relatively long-lived spin density fluctuations in the nearly ferromagnetic itinerant d band of the metal.²⁸

The absolute resistivity of the pure-Pd sample, measured at the ice point, provides a check on the measured area-to-length ratio; the value of $9.81 \pm 0.05 \mu\Omega \text{ cm}$ obtained here compares well with previous values.²⁹

B. PdFe Magnetoresistance

In Fig. 3 the incremental resistivity $\Delta\rho(H, T) = \rho_{\text{alloy}}(H, T) - \rho_{Pd}(H=0, T)$ of the Pd-0.78-at. % Fe sample is plotted as a function of temperature up to 15 K, in zero applied magnetic field, and in fields of 9.7, 25, and 59 kOe.

Long and Turner¹⁸ have given the following expression for the incremental resistivity of the alloy in zero magnetic field at temperatures $T \ll T_c$:

$$\Delta\rho(H=0, T) = \rho_0 c + Bc^{-1/2} T^{3/2}. \quad (2)$$

The temperature-independent term $\rho_0 c$ arises from the elastic part of the exchange scattering and (elastic) charge scattering, while the temperature-dependent term has contributions from s -electron spin-flip scattering from collective excitations, from the temperature dependence of the non-spin-flip (elastic) part of the exchange scattering, and from interference effects between exchange and charge (potential) scattering. Previous measurements on this sample²⁴ in zero magnetic field have shown that Eq. (2) provides [a good description of the data up to around 12 K (the Curie temperature T_c of the alloy was estimated to be $(32.6 \pm 0.3 \text{ K})$].³⁰ These measurements also estimated ρ_0 at $1.9 \mu\Omega \text{ cm}/\text{at. \% Fe}$, and the coefficient of the $T^{3/2}$ term ($Bc^{-1/2}$) for the 0.78-at. % Fe alloy as $1.36 \pm 0.2 \times 10^{-3} \mu\Omega \text{ cm}/\text{K}^{3/2}$; the concentration dependence

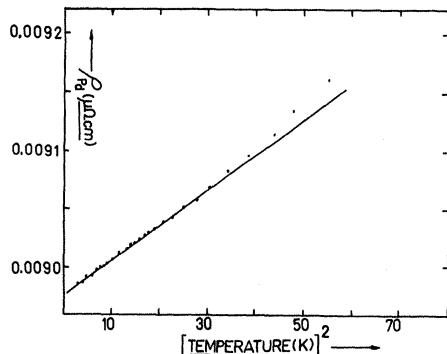


FIG. 2. The resistivity of the Pd sample $\rho_{Pd}(T)$ ($\mu\Omega \text{ cm}$) plotted against [temperature (K)]².

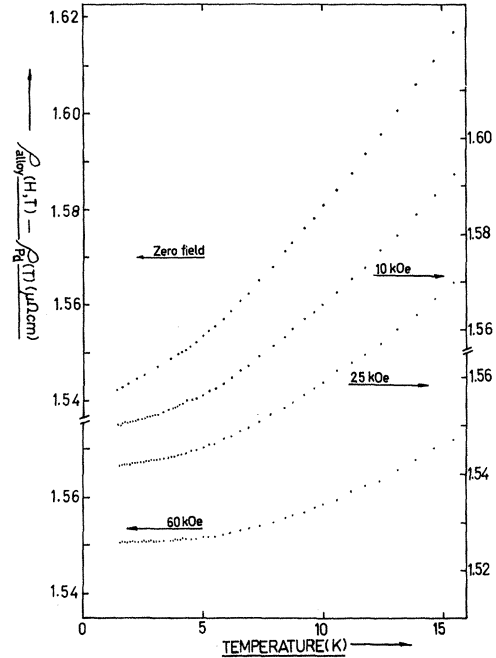


FIG. 3. The incremental resistivity of the Pd-0.78-at. % Fe sample [$\rho_{\text{alloy}}(H, T) - \rho_{Pd}(T)$] ($\mu\Omega \text{ cm}$) measured in various applied fields and plotted against temperature (K).

of this $T^{3/2}$ term is not that predicted in Eq. (2); the origin of this discrepancy is discussed elsewhere.^{24, 25, 31} Fitting Eq. (2) to the present data over the temperature range 1.4–12 K yields $\rho_0 \approx 1.9(7) \mu\Omega \text{ cm}/\text{at. \% Fe}$ while the $T^{3/2}$ term agrees within experimental error with that previously quoted. The increase in the estimated value for ρ_0 could simply reflect the effects of thermal cycling.

The extension of the previous model to include the effects of an applied magnetic field H yields (at temperatures $T \ll T_c$, and in those alloys where the charge scattering is much stronger than the exchange scattering) the following expression for²¹ $\Delta\rho(H, T)$:

$$\Delta\rho(H, T) = \alpha c (V^2 - 3J^2 S^2) + \frac{\alpha c J^2 S \Gamma(\frac{3}{2}) (\frac{\Omega}{N}) (\frac{k_B T}{D})^{3/2}}{2\pi^2} \times \left(4 \sum_{n=1}^{\infty} \frac{(e^{-t})^n}{n^{3/2}} - \sum_{n=1}^{\infty} \frac{(-e^{-t})^n}{n^{3/2}} \right). \quad (3)$$

The V is the spin-independent screened Coulomb potential arising from the charge difference between impurity and host; J and S are as previously defined. $\Gamma(x)$ is the appropriate gamma function, Ω is the atomic volume, and N is the number of atoms in that volume; k_B is Boltzmann's constant. In the long-wavelength limit the energy E_q of a collective excitation of wave vector q in an applied field H is written³²

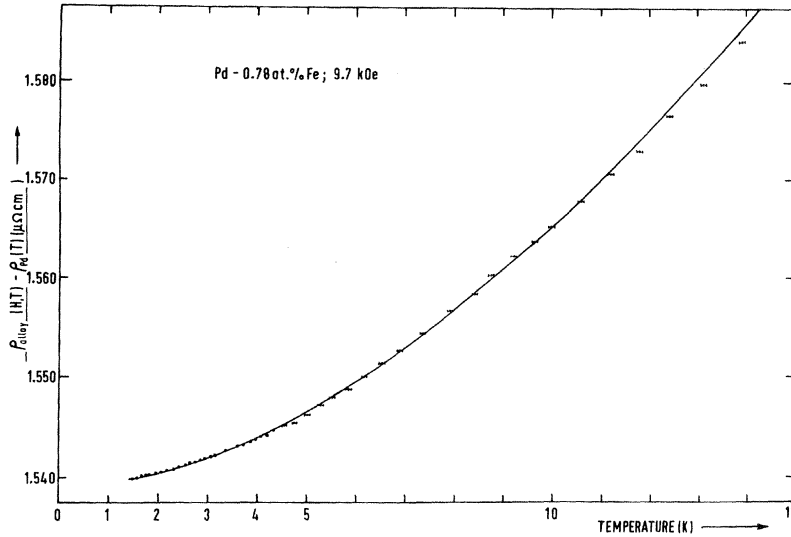


FIG. 4. The incremental resistivity of the Pd-0.78-at.% Fe sample [$\rho_{\text{alloy}}(H, T) - \rho_{\text{Pd}}(T)$] ($\mu\Omega \text{ cm}$) in a field of 9.7 kOe plotted against temperature. The curve through the data points is calculated from Eq. (3).

$$E_q = Dq^2 + g\mu_B H. \quad (4)$$

The μ_B is the Bohr magneton and g is the splitting factor. This equation defines the acoustic spin-wave stiffness constant D . (It is assumed to be independent of temperature; this assumption will be discussed later.) In Eq. (3), $t = g\mu_B H/k_B T$ and

$$\alpha = 3\pi m^* \Omega / 2e^2 \hbar N E_F. \quad (5)$$

Here m^* is the conduction-electron effective mass and E_F labels the Fermi energy. Assuming that the conductivity is dominated by s electrons in a parabolic band with $m^*/m = 2.2$,^{19,20} then $E_F = 1.33$ eV and $\alpha = 6.52 \mu\Omega \text{ cm}/(\text{eV})^2$ at.%. Since Eq. (3) is a direct extension of Eq. (2), its range of validity (in temperature) in an applied field H should be the same as the range of validity of the $T^{3/2}$ form for the incremental resistivity in zero applied field.

In zero applied magnetic field ($t=0$), not unexpectedly, the $T^{3/2}$ temperature dependence of Eq. (2) is recovered from (3), with the coefficient of this term (in the limit of $|V^2| \gg |J^2|$) being given by

$$T^{3/2} \text{ coefficient} = \left(\frac{\Omega}{N}\right) \left(\frac{k_B}{D}\right)^{3/2} [4\Gamma(\frac{3}{2})G(\frac{3}{2}) + F_{1/2}(0)] \\ \times \left(\frac{\Delta\rho(H=0, T_c) - \Delta\rho(H=0, T=0)}{2\pi^2(1+4S)}\right). \quad (6)$$

In arriving at Eq. (6), use has been made of the following expression for J^2 ,³³ valid in the limit $|V|^2 \gg |J|^2$:

$$J^2 = \frac{\Delta\rho(H=0, T_c) - \Delta\rho(H=0, T=0)}{\alpha c S (1+4S)}. \quad (7)$$

In Eq. (6), $G(x)$ and $F_k(x)$ are the appropriate Riemann zeta and Fermi-Dirac functions, respectively. The zero-field measurements enable $\alpha c(V^2 - 3J^2 S^2)$ to be estimated [this is simply

$\Delta\rho(H=0, T=0)$], while measurement of the $T^{3/2}$ coefficient allows estimates of D to be made via Eq. (6); for the model used here—single-band conduction in which the carriers are treated in an effective-mass approximation—this estimate of D depends only on the assumed value for S . [It does, however, differ by a factor of $c^{2/3}$ from values obtained using conventional analysis^{34,35}; the origin of this difference is discussed elsewhere³⁶; the various estimates for D are otherwise in good agreement. This difference in definition does not affect the analysis of the magnetoresistance data, since here one essentially considers the modification of the measured (zero-field) $T^{3/2}$ coefficient by the field-dependent sums of Eq. (3).] The calculation of the incremental resistivity $\Delta\rho(H, T)$ in a field H , via Eq. (3), is then straightforward.

In Fig. 4 the experimental data points in an applied field of 9.7 kOe are fitted using Eq. (3) in conjunction with the measured zero-field $T^{3/2}$ coefficient. The only adjustable parameter is the splitting factor g in Eq. (4); the curve shown is for $g=2$. The experimental data are well fitted up to about 12 K, the expected range of validity of Eq. (3). No mention has yet been made of the effects of "normal" magnetoresistance (designated ρ_{Kohler}) due to the cyclotron curvature of the conduction-electron orbits in an applied magnetic field. Kohler³⁷ has indicated that

$$\frac{\rho_{\text{Kohler}}}{\rho_{\text{alloy}}(H=0, T)} = f\left(\frac{H}{\rho(H=0, T)}\right), \quad (8)$$

with f representing some general function. The dual conditions of $T \ll T_c$ and $|V|^2 \gg |J|^2$ mean that over the temperature range of interest $\rho(H=0, T)$ is not a rapidly varying function of temperature. For the PdFe alloy examined here

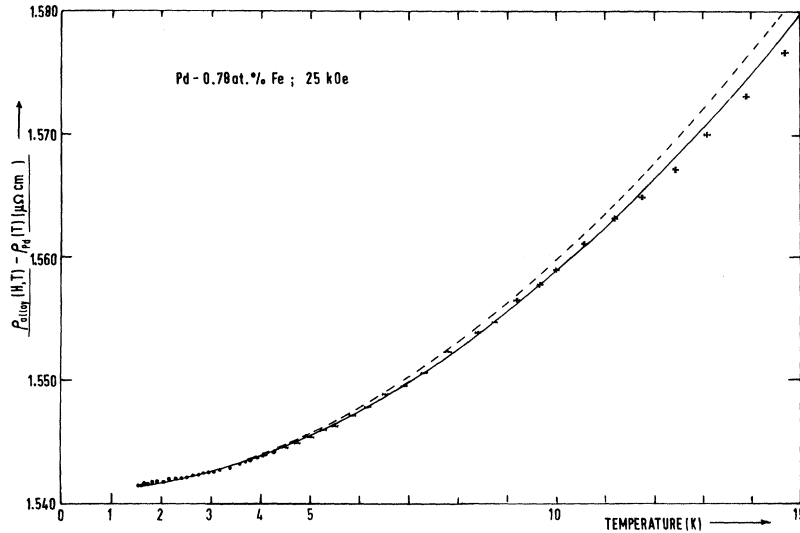


FIG. 5. The incremental resistivity of the Pd-0.78-at.% Fe sample [$\rho_{\text{alloy}}(H, T) - \rho_{\text{Pd}}(T)$] ($\mu\Omega \text{ cm}$) in a field of 25 kOe plotted against temperature. The two curves are calculated from Eq. (3) (see text).

$$\frac{\rho_{\text{alloy}}(H=0, T=12 \text{ K}) - \rho_{\text{alloy}}(H=0, T=0)}{\rho_{\text{alloy}}(H=0, T=0)} < 4\% .$$

In a fixed field, ρ_{Kohler} is thus regarded as being constant in the temperature interval up to 12 K; correction for the normal magnetoresistance consequently amounts simply to a uniform shift of the data. The magnitude of ρ_{Kohler} is taken as that shift necessary to make the experimental data and the theoretical calculation agree at 1.5 K; these estimates are listed in Table I. They appear to be in agreement with measurements made by Arajs, Dunmyre, and Dechter³⁸ on PdEr alloys, where the magnetoresistance seems to be dominated by the "normal" contribution, spin-disorder scattering apparently making a negligible contribution. For a Pd-0.5-at.% Er alloy with $\rho(H=0, T=0) = 1.58 \mu\Omega \text{ cm}$ (close to the value of $1.54 \mu\Omega \text{ cm}$ for the PdFe alloy investigated here), $\Delta\rho(H=60 \text{ kOe}, T=4.2 \text{ K})$ was measured at $0.016 \mu\Omega \text{ cm}$.

Figure 5 shows $\Delta\rho(H, T)$, measured in an applied field of 25 kOe, plotted against temperature. The dashed curve in this figure is calculated from Eq. (3) using $H=25 \text{ kOe}$, the measured $T^{3/2}$ coefficient, and putting $g=2$. The fit is not good; we thus conclude that D is field dependent. Similar conclusions have been reached from recent analyses of magnetization and specific-heat measurements on PdFe alloys of comparable concentration.^{35,39} To account for this variation with field, a modified $T^{3/2}$ coef-

ficient is fed into the magnetoresistance calculation via Eqs. (3) and (6). The full curve in Fig. 5 is calculated using the appropriate field, $g=2$, and a modified $T^{3/2}$ coefficient of $1.29 \times 10^{-3} \mu\Omega \text{ cm}/\text{K}^{3/2}$; the modified $T^{3/2}$ coefficients used to fit the experimental data in various applied fields are listed in Table II.

The values of D associated with these modified coefficients, calculated from Eq. (6), are also listed. In calculating these values of D the impurity spin S has been taken to be 4.5. This value derives from fitting recent magnetoresistance data on a Pd-0.1-at.% Fe alloy in the temperature range 1.5–10 K and in fields up to 60 kOe ($T_C = 0.78 \text{ K}$ for this alloy), using an $s-d$ model.⁴⁰ This value for S is somewhat higher than the value required by Maley, Taylor, and Thompson⁴¹ ($S \approx 3.9$) to fit their Mössbauer data on dilute PdFe alloys [although the g values (2.9) deduced from both sets of measurements are in excellent agreement].

The magnetoresistance data in 59 kOe are plotted as a function of temperature in Fig. 6; the dashed curve in this figure is again the calculated variation using the measured $T^{3/2}$ coefficient, whereas the full curve uses the modified coefficient listed

TABLE I. Estimated Kohler terms for Pd-0.78-at.% Fe.

Field (in kOe)	Kohler term (in $\mu\Omega \text{ cm}$)
9.7	< 0.0001
25	0.0056
59	0.0157

TABLE II. Parameters deduced for Pd-0.78-at.% Fe from the fitting procedures. All fits were done with $g=2.00$.

Field (in kOe)	Modified $T^{3/2}$ coefficients (in $10^3 \mu\Omega \text{ cm}/\text{K}^{3/2}$)	Acoustic spin-wave stiffness (in $\text{K} \text{ \AA}^2$)
0	1.36	14.9(3)
9.7	1.35	15.0(0)
25	1.29	15.4(7)
59	1.13	16.8(9)

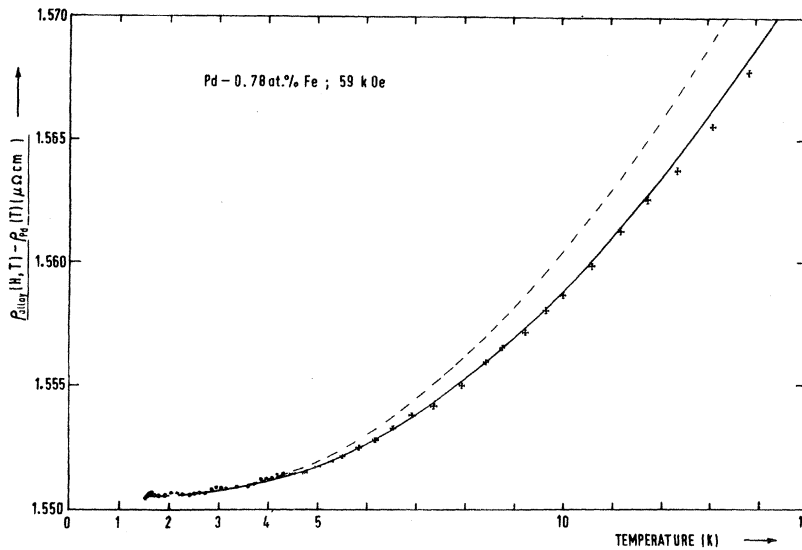


FIG. 6. The incremental resistivity of the Pd-0.78-at.% Fe sample [$\rho_{\text{alloy}}(H, T) - \rho_{\text{Pd}}(T)$] ($\mu\Omega \text{ cm}$) in a field of 59 kOe plotted against temperature. See text for the origin of the two curves shown.

in Table II.

When D is field dependent, there is an extra contribution to $\Delta\rho(H, T)$ as calculated in Eq. (3). Smith, Gardner, and Montgomery³⁵ have considered the modification of the magnetization resulting from a field-dependent acoustic spin-wave stiffness constant; in the present context the lowest-order contribution (in temperature) to $\Delta\rho(H, T)$ from this source is simply the term

$$\frac{\alpha c J^2 S \Gamma(\frac{5}{2})}{2\pi^2 g \mu_B} \left(\frac{\Omega}{N}\right) \left(\frac{k_B T}{D}\right)^{5/2} \frac{\partial D}{\partial H} \times \left(4 \sum_{n=1}^{\infty} \frac{(e^{-t})^n}{n^{5/2}} - \sum_{n=1}^{\infty} \frac{(-e^{-t})^n}{n^{5/2}}\right). \quad (9)$$

Clearly, in zero applied field ($t=0$) this supplies a $T^{5/2}$ term; thus, as long as we confine our fitting procedure to the temperature region where the $T^{3/2}$ expansion is valid, we can simply use Eq. (3) to fit the data taken in an applied field, leaving out the contribution in Eq. (9) above. This is, in fact, the approach used.

C. PdCo Magnetoresistance

The measured incremental resistivity $\Delta\rho(H, T)$ of the Pd-0.73-at.% Co alloy, in zero field and in fields of 9.7, 24.8, and 58.5 kOe, is plotted in Fig. 7 as a function of temperature. An analysis of these data along the lines followed for the PdFe system was attempted.

The zero-field measurements are well represented up to about 12 K by Eq. (2) [T_C for this alloy is (27.5 ± 0.3) K], with ρ_0 estimated at $1.42 \mu\Omega \text{ cm/at.}\%$ Co and the coefficient of the $T^{3/2}$ term at $3.52 \times 10^{-3} \mu\Omega \text{ cm/K}^{3/2}$. These estimates are in good agreement with previous measurements.²⁵ Figure 8 shows in more detail the experimental data in 9.7 kOe; the dashed curve represents the

variation of $\Delta\rho(H, T)$ calculated from Eq. (3) using $g=2$, the measured $T^{3/2}$ coefficient and the appropriate field. Unlike the situation in PdFe alloys of comparable concentration and in the same applied field, this calculated variation does not fit the experimental data (it clearly lies well below the experimental points). Within the present scheme of analysis we can attempt to fit the data either by reducing D below its zero-field value, or by reducing the splitting factor g describing the field-in-

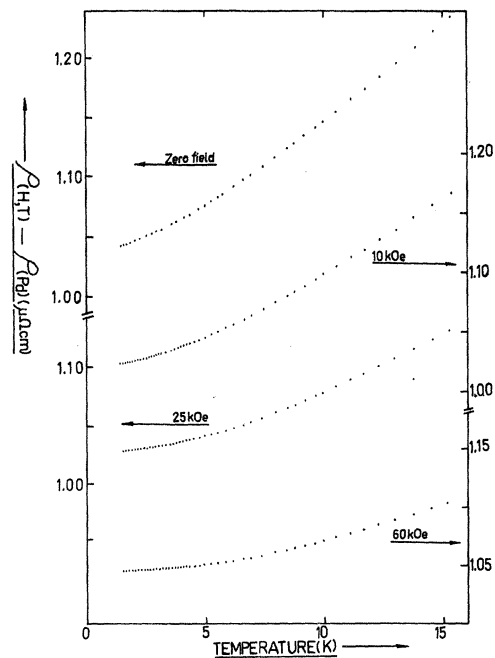


FIG. 7. The incremental resistivity of the Pd-0.73-at.% Co sample [$\rho(H, T) - \rho_{\text{Pd}}(T)$] ($\mu\Omega \text{ cm}$) in various applied fields plotted against temperature.

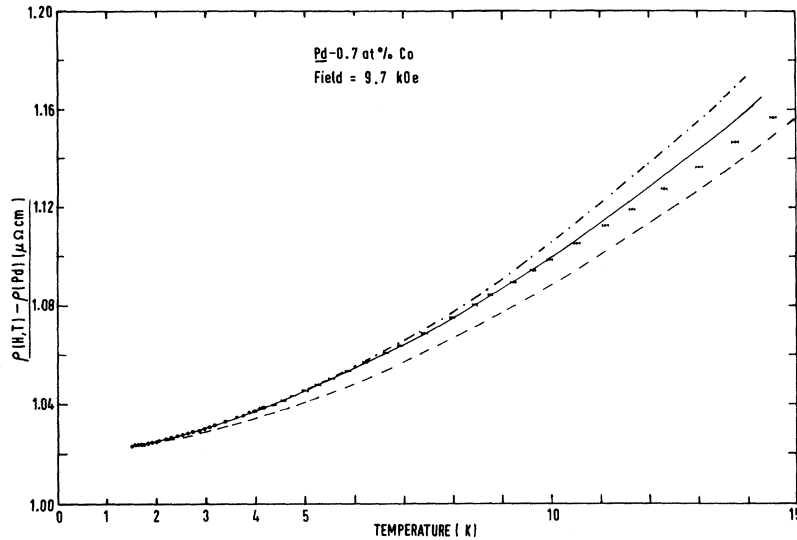


FIG. 8. The incremental resistivity of the Pd-0.73-at.% Co sample [$\rho(H, T) - \rho_{Pd}(T)$] ($\mu\Omega \text{ cm}$) in a field of 9.7 kOe plotted against temperature. The curves are explained in the text.

duced energy gap in the magnon spectrum at $q=0$. The dot-dash-dot curve in Fig. 8 is the best calculated fit obtainable with $g=2$ and a reduced D [it corresponds to a modified $T^{3/2}$ coefficient of $4.40 \times 10^{-3} \mu\Omega \text{ cm/K}^{3/2}$, and an associated D of $9.9(5) \text{ K}\text{\AA}^2$. The latter is calculated using an impurity spin of $S=4.7$, obtained from the analysis of recent magnetoresistance data on a Pd-0.098-at.% Co alloy⁴⁰]. The solid curve in this figure is that calculated from Eq. (3) using the measured (zero-field) $T^{3/2}$ coefficient [the associated $D=11.6(8) \text{ K}\text{\AA}^2$] with g reduced to 0.8. Not only does this latter prescription provide the best fit to the data, but its range of validity also corresponds to that of the $T^{3/2}$ expansion in zero field; in addition, the previous analysis of the PdFe data suggested that D does not reduce below its zero-field value, the latter also being applicable to fitting the data in an applied field of 9.7 kOe. It was therefore decided

to fit the data with a splitting factor $g=0.8$.

The data taken in fields of 24.8 and 58.5 kOe are reproduced in Figs. 9 and 10, respectively, along with the calculated variation of $\Delta\rho(H, T)$. In both figures the dashed curve represents the results of calculations using $g=0.8$ and the measured $T^{3/2}$ coefficient, whereas the solid curves use the modified coefficients listed in Table III. It is clear that we are again forced to conclude that D is field dependent. Wheeler⁴² has measured the low-temperature specific heat of several dilute PdCo alloys in the ferromagnetic phase, and observes a $T^{3/2}$ (spin-wave) contribution. Wheeler's estimates of the coefficient of this term are admittedly unreliable, but for an 0.5-at.% Co alloy the acoustic spin-wave stiffness constant associated with the (range of) coefficient quoted is $27\text{--}31 \text{ K}\text{\AA}^2$. This is, at least, in order-of-magnitude agreement with the estimates obtained in this investigation.

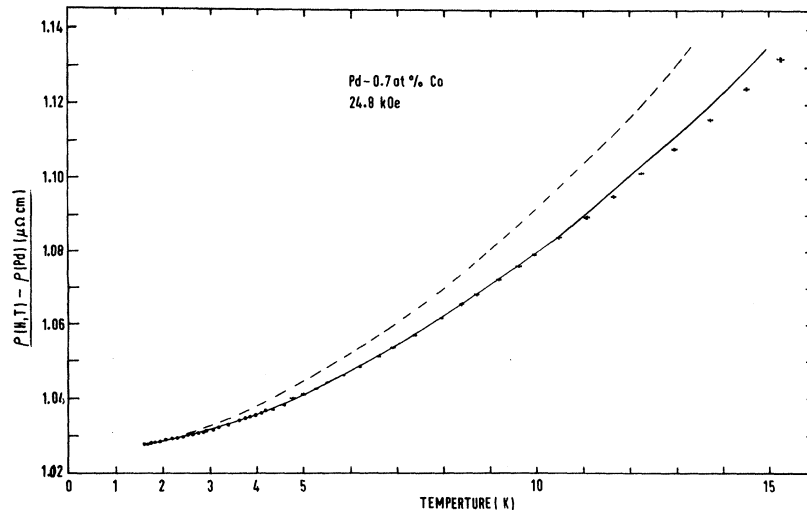


FIG. 9. The incremental resistivity of the Pd-0.73-at.% Co sample [$\rho(H, T) - \rho_{Pd}(T)$] ($\mu\Omega \text{ cm}$) in a field of 24.8 kOe plotted against temperature. The curves are explained in the text.

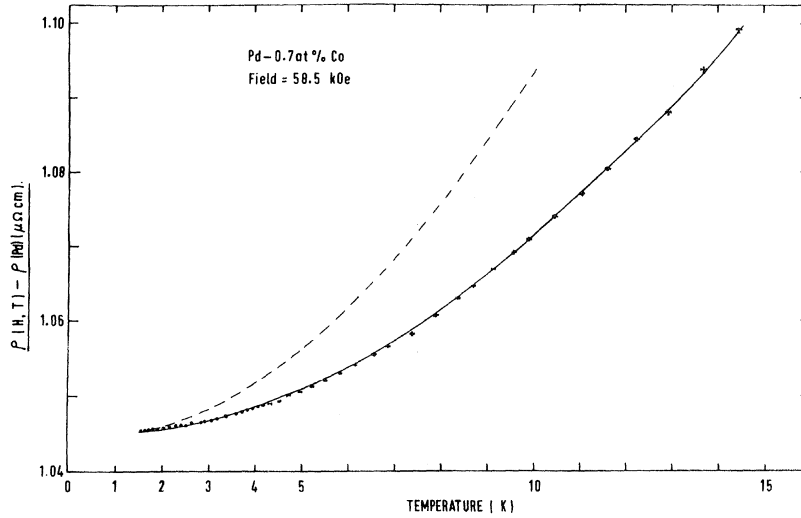


FIG. 10. The incremental resistivity of the Pd-0.73-at. % Co sample $[\rho(H, T) - \rho_{Pd}(T)]$ ($\mu\Omega$ cm) in a field of 58.5 kOe plotted against temperature. The curves are explained in the text.

Estimates of the Kohler terms for this alloy are listed in Table IV.

D. Field-Dependent Acoustic Spin-Wave Stiffness Constants

In Fig. 11 the dimensionless quantity $[D(H) - D(0)] \cdot D(0)^{-1}$ for Pd-0.78-at. % Fe is plotted against the applied field H ; the figure shows that this dimensionless ratio is roughly proportional to the applied field, in agreement with the conclusions of Smith *et al.*³⁵ The latter authors estimate the coefficient of proportionality as $(14 \pm 4) \times 10^{-3}/\text{kOe}$, which is about a factor of 5 larger than that estimated in Fig. 11 for this investigation, $(2.3 \pm 0.4) \times 10^{-3}/\text{kOe}$.

Realistic calculations of the acoustic spin-wave stiffness in a binary alloy are difficult to perform. Using the dynamical model previously discussed and an effective-mass treatment of a single d band, the analysis of Doniach and Wohlfarth leads to the following expression for D (see Ref. 18):

$$D = \frac{2(J_{d \text{ local}} \chi_\rho)^2}{27(1 + J_{d \text{ local}} \chi_\rho)} \frac{cS}{zm_d^*}. \quad (10)$$

Here z is the number of d holes per atom, m_d^* is the effective mass of the d holes, and χ_ρ is the

TABLE III. Parameters deduced for Pd-0.73-at. % Co from the fitting procedures. These fits were obtained with $g = 0.8$.

Field (in kOe)	Modified $T^{3/2}$ coefficients (in $10^3 \mu\Omega \text{ cm}/\text{K}^{3/2}$)	Acoustic spin-wave stiffness (in $\text{K}\text{\AA}^2$)
0	3.52	11.6(1)
9.7	3.48	11.6(8)
24.8	2.80	13.4(6)
58.5	1.90	17.4(3)

static exchange-enhanced susceptibility of the host's d band. Equation (10) is valid in the limit $q \ll [k_F(\uparrow) - k_F(\downarrow)]$, with $k_F(\uparrow)$ and $k_F(\downarrow)$ being the Fermi momenta of spin-up and -down d holes.¹⁷ However, in Ref. 16, it is claimed that the relevant range of q is $k_F(\uparrow) - k_F(\downarrow) \ll q \ll k_F(\uparrow), k_F(\downarrow)$, consequently (see Long and Turner¹⁸),

$$D = 2J_{d \text{ local}}^2 SN(0)c/3[1 - IN(0)]^2, \quad (11)$$

where $N(0)$ is the total unenhanced density of d states at the Fermi level, and I is the intra-atomic Coulomb repulsion between d electrons. Equation (11) may simply be rewritten as

$$D = 2J_{d \text{ local}}^2 \chi_\rho Sc/3K_0^2 \mu_B, \quad (12)$$

with the enhancement factor $K_0^{-2} = [1 - IN(0)]^{-1}$. It is clear that over the relevant temperature range neither Eq. (10) nor (12) suggests that D will be temperature dependent. This accords with the present observations, and with the analysis of magnetization,^{35,39} specific heat,^{39,43} NMR,⁴⁴ and neutron diffraction³⁴ studies on PdFe alloys of comparable concentration. The only contrary result comes from the analysis by Oder⁴⁵ of magnetization measurements on a Pd-0.1-at. % Fe alloy. In the approach of Doniach and Wohlfarth,¹⁸ the saturation moment μ_S per iron atom is given by

$$\mu_S = g\mu_B S(1 + J_{d \text{ local}} \chi_\rho). \quad (13)$$

We now use this expression in conjunction with Eqs. (10) and (12) to examine the various possible

TABLE IV. Estimated Kohler terms for Pd-0.73-at. % Co.

Field (in kOe)	Kohler term (in $\mu\Omega \text{ cm}$)
9.7	< 0.0001
24.8	0.0030
58.5	0.0082

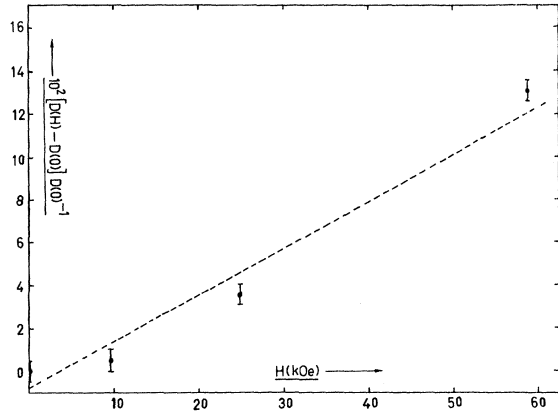


FIG. 11. The dimensionless ratio $[D(H) - D(0)] \cdot D(0)^{-1}$ plotted against applied field H (kOe). The vertical error bars correspond to a $\pm 1\%$ variation in the estimated $T^{3/2}$ coefficient.

sources of field dependence in D .

1. Field Dependence of $J_{d \text{ local}} \chi_p$

Following Smith *et al.*³⁷ we assume that at typical applied fields z and m_d^* appearing in Eq. (10) are field independent, and initially attribute a field dependence solely to the product $J_{d \text{ local}} \chi_p$. This leads, via Eqs. (10) and (13), to³⁵

$$\frac{\partial \ln D}{\partial H} = (J_{d \text{ local}} \chi_p) \frac{\partial \ln \mu_S}{\partial H}. \quad (14)$$

$J_{d \text{ local}} \chi_p$ may be estimated from the measured g value in the paramagnetic phase of alloys containing less than 0.1-at. % Fe^{40, 41}; $g_{\text{eff}} = 2.9$ implies $J_{d \text{ local}} \chi_p = 0.45$. The obvious limitation of this estimate lies in the field independence of g_{eff} , and hence $(J_{d \text{ local}} \chi_p)$, in the paramagnetic regime; it is, however, the most realistic estimate available. Using the field variation of D estimated in Fig. 11 from the magnetoresistance data, Eq. (14) implies a 23% increase of μ_S (for the 0.78-at. % Fe alloy) in 40 kOe over its zero-field value.

In the case of the Cole-Turner expression for D [Eq. (13)], assuming that the enhancement factor K_0^{-2} is field independent over the field range of interest here, an analogous approach yields

$$\frac{\partial \ln D}{\partial H} \geq \frac{\partial \ln \mu_S}{\partial H}. \quad (15)$$

Application of Eq. (15) for these same data implies an increase in μ_S of $\leq 9\%$ for the 0.78-at. % Fe alloy in 40 kOe. Analysis of the magnetization data³⁵ yields an 8% increase in μ_S in 40 kOe for an 0.53-at. % Fe alloy, and a 6% increase for a 1-at. % Fe alloy in the same field.

2. Field Dependence of S

Using the assumptions of Sec. III D⁴⁶

regarding the field independence of z , m_d^* , and K_0^{-2} , but now attributing a field dependence to S rather than $J_{d \text{ local}} \chi_p$, both expressions yield

$$\frac{\partial \ln D}{\partial H} = \frac{\partial \ln \mu_S}{\partial H}, \quad (16)$$

i. e., both models suggest a 9% increase in μ_S (in 40 kOe for the 0.78-at. % Fe alloy) from the field variation in D estimated from the magnetoresistance data.

We conclude this section with a brief discussion of the PdCo results. The field dependence of D , derived from fitting the magnetoresistance data (Table III), does not appear to vary in a systematic manner with applied magnetic field. This, however, could simply reflect the restrictions placed on D and g in our fitting procedure, viz., we required $D(H = 9.7 \text{ kOe}) \approx D(H = 0)$ —as was the case for the magnetoresistance data in PdFe—consequently, needing $g = 0.8$. However, we could have allowed $D(H = 9.7 \text{ kOe}) > D(H = 0)$, but then we would have required $g < 0.8$. In any event the choice of $g = 0.8$ still requires $D(H > 9.7 \text{ kOe})$ to be field dependent.

Using Eqs. (15) or (16), which appear to correlate the field dependence of D with μ_S for PdFe quite well, μ_S should increase with applied field in PdCo. The nonsystematic variation of D with H means that we can only make a rough estimate of this increase; for the variation of D found in this investigation, μ_S should increase by approximately 30% in a 40-kOe field for this 0.73-at. % Co alloy.

IV. SUMMARY

Magnetoresistance data on a Pd-0.78-at. % Fe alloy for temperatures in the range 1.5–12 K and in magnetic fields up to 60 kOe, appear to be well fitted by the inclusion of an applied field in the model of Long and Turner,¹⁸ the latter satisfactorily explaining the zero-field properties of this system. These data are consistent with a splitting factor g —describing the field-induced energy gap in the magnon spectrum at $q = 0$ —being 2.0, but require the acoustic spin-wave stiffness D to be field dependent. The field dependence of D , estimated from the magnetoresistance data, is reasonably well represented by $[D(H) - D(0)] \cdot D(0)^{-1} = \beta H$, in agreement with the recent analysis of magnetization data,³⁵ but with β about five times smaller than the value estimated from this latter analysis.

An attempt to correlate the field dependence of D with that in the saturation impurity moment μ_S within the framework of the Doniach-Wohlfarth model,¹⁶ by attributing a field dependence to $(J_{d \text{ local}} \chi_p)$ leads to a predicted field variation in μ_S , which is some three times larger than that ob-

served experimentally. Similar conclusions were reached by Smith *et al.*,³⁵ although it should be pointed out that the numerical values chosen for β and $(J_{d \text{ local}} \chi_p)$ were significantly different from those used in the present analysis. However, the field variation of D and μ_S correlate well if the field dependence is attributed in the Doniach-Wohlfarth model to the impurity spin S ; in the Cole-Turner model,¹⁷ attributing a field variation to either S or $(J_{d \text{ local}} \chi_p)$ reproduces the field dependence of μ_S from the observed field dependence of D .

Magnetoresistance measurements on a Pd-0.73-at. % Co alloy can only be fitted within the present scheme of analysis by assuming a splitting factor g significantly different from 2.0. Magnetization measurements in various applied fields on this class of alloys in the ferromagnetic phase would clearly be useful in clarifying their properties. The field variation of D again required to fit the magnetoresistance data implies a field variation in μ_S , the field dependence being roughly estimated as a 30% increase in μ_S in a 40-kOe field over its zero-field value.

*This work has been sponsored in part by the Air Force Materials Laboratory through the European Office of Aerospace Research, United States Air Force, under contract F61052-68-C-0011. The final sections of this work at the University of Manitoba were supported by the National Research Council of Canada under Grant No. A6407.

¹J. Crangle, *Phil. Mag.* **5**, 335 (1960).

²R. M. Bozorth, P. A. Wolff, D. D. Davis, V. B. Compton, and J. H. Wernick, *Phys. Rev.* **122**, 1157 (1961).

³A. M. Clogston, B. T. Matthias, M. Peter, H. J. Williams, E. Corenzwit, and R. C. Sherwood, *Phys. Rev.* **125**, 541 (1962).

⁴J. Crangle and W. R. Scott, *J. Appl. Phys.* **36**, 921 (1965).

⁵See, for example, R. Segnan, *Phys. Rev.* **160**, 404 (1967).

⁶K. Yosida, *Phys. Rev.* **106**, 893 (1957).

⁷This argument applies to the d -band polarization; the relevant exchange interaction is between the impurity spins and the d electrons, and is characterized by the exchange coupling $J_d \text{ local}$.

⁸B. Giovaninni, M. Peter, and J. R. Schrieffer, *Phys. Rev. Letters* **12**, 736 (1964).

⁹D. J. Kim and B. B. Schwartz, *Phys. Rev. Letters* **20**, 201 (1968).

¹⁰G. G. Low and T. M. Holden, *Proc. Phys. Soc. (London)* **89**, 119 (1966).

¹¹W. L. Trousdale, G. Longworth, and T. A. Kitchens, *J. Appl. Phys.* **38**, 922 (1967).

¹²B. D. Dunlap and J. G. Dash, *Phys. Rev.* **155**, 406 (1967).

¹³P. Rhodes and E. P. Wohlfarth, *Proc. Roy. Soc. (London)* **273A**, 247 (1963).

¹⁴T. Moriya, *Progr. Theoret. Phys. (Kyoto)* **34**, 329 (1965).

¹⁵P. W. Anderson, *Phys. Rev.* **124**, 41 (1961).

¹⁶S. Doniach and E. P. Wohlfarth, *Proc. Roy. Soc. (London)* **295A**, 442 (1967).

¹⁷H. S. D. Cole and R. E. Turner, *J. Phys. C* **2**, 124 (1969).

¹⁸P. D. Long and R. E. Turner, *J. Phys. C* **2**, S127 (1970).

¹⁹J. J. Vuillemin and M. G. Priestley, *Phys. Rev. Letters* **14**, 307 (1965).

²⁰J. J. Vuillemin, *Phys. Rev.* **144**, 396 (1966).

²¹G. Williams, *Solid State Commun.* **9**, 1451 (1970).

²²M. Kohler, *Physik* **126**, 495 (1949).

²³J. S. Dugdale and Z. S. Basinski, *Phys. Rev.* **157**, 552 (1967).

²⁴G. Williams and J. W. Loram, *J. Phys. Chem. Solids*

30, 1827 (1969).

²⁵G. Williams, *J. Phys. Chem. Solids* **31**, 529 (1970).

²⁶J. W. Loram, T. E. Whall, and P. J. Ford, *Phys. Rev. B* **2**, 857 (1970).

²⁷A. I. Schindler and M. J. Rice, *Phys. Rev.* **164**, 759 (1967).

²⁸P. Lederer and D. L. Mills, *Phys. Rev.* **165**, 837 (1968).

²⁹L. F. Bates and P. B. Unstead, in *Proceedings of the International Conference on Magnetism, Nottingham 1964* (The Institute of Physics and The Physical Society, London, 1965).

³⁰ T_C was taken as the temperature at which a sharp change in slope of $\Delta\rho(H=0, T)$ occurred. Recently M. P. Kawatra, J. I. Budnick, and J. A. Mydosh [*Phys. Rev. B* **2**, 1587 (1970)] have suggested that T_C should be taken as the temperature at which $d[\Delta\rho(H=0, T)]/dT$ is a maximum. This criterion does not greatly affect the estimated T_C for alloys of the concentration investigated here, nor is this estimate of direct importance to the subsequent analysis.

³¹G. Williams and J. W. Loram, *Solid State Commun.* **7**, 1261 (1969).

³²The field that enters Eq. (4) should include contributions from anisotropy and demagnetizing fields. The work of D. M. S. Bagguley, W. A. Crossley, and J. Liesegang [*Proc. Phys. Soc. (London)* **90**, 1047 (1967)] has shown the former to be very small, whereas for the present sample geometry, the latter should be vanishingly small.

³³K. Yosida, *Phys. Rev.* **107**, 396 (1957).

³⁴M. W. Stringfellow, *J. Phys. C* **1**, 1699 (1968).

³⁵T. F. Smith, W. E. Gardner, and H. Montgomery, *J. Phys. C* **1**, S370 (1970).

³⁶G. Williams and J. W. Loram, *J. Phys. F* (to be published)

³⁷M. Kohler, *Ann. Phys. (Leipzig)* **32**, 211 (1938).

³⁸S. Arajs, G. R. Dunmyre, and S. J. Dechter, *Phys. Status Solidi* **18**, 505 (1966).

³⁹T. F. Smith, W. E. Gardner, and J. I. Budnick, *Phys. Letters* **27A**, 326 (1968).

⁴⁰A. D. C. Grassie, G. A. Swallow, G. Williams, and J. W. Loram, *Phys. Rev. B* (to be published).

⁴¹M. P. Maley, R. D. Taylor, and J. L. Thompson, *J. Appl. Phys.* **38**, 1249 (1967).

⁴²J. C. G. Wheeler, *J. Phys. C* **2**, 135 (1969).

⁴³B. W. Veal and J. A. Rayne, *Phys. Rev.* **135**, 442 (1964).

⁴⁴S. Skalski, J. I. Budnick, and J. Lechaton, *J. Appl. Phys.* **39**, 965 (1968).

⁴⁵R. R. Oder, *J. Appl. Phys.* **40**, 1204 (1969).

⁴⁶If the analysis of Secs. III D 1 and 2 is applied in an

attempt to correlate any temperature dependence in D with that in μ_S , the temperature independence of the one

implies a temperature independence in the other, as observed experimentally.

Neutron Diffraction and Magnetic Structure of CsMnCl_3

M. Melamud, J. Makovsky, and H. Shaked

Nuclear Research Centre—Negev P. O. B. 9001, Beer-Sheva, Israel

(Received 30 November 1970)

The room-temperature (paramagnetic) structure of CsMnCl_3 is verified by neutron powder diffraction studies. This compound is found to be a perovskite-related compound (the nine-layer structure) which belongs to the trigonal space group $D_{3d}^5-R\bar{3}m$. The compound is antiferromagnetic below 67 °K; its magnetic structure is deduced from its neutron diffraction pattern at liquid-helium temperature. This structure is of the G type with a \vec{k} vector $(\frac{1}{2}, \frac{1}{2}, \frac{1}{2})$ related to the rhombohedral crystallographic lattice. The spin direction is perpendicular to the body diagonal of the rhombohedral unit cell. The magnetic symmetry is monoclinic, belonging to the space group $C_{2c}2/m$. A dipolar energy calculation confirms the spin direction found. A magnetic moment of $(5.5 \pm 0.5)\mu_B$ is calculated for the Mn^{+2} ions.

INTRODUCTION

The compound CsMnCl_3 was prepared¹⁻⁵ and investigated by x rays,^{2,5} nuclear magnetic resonance (NMR),⁶ antiferromagnetic resonance (AFMR),^{7,8} and ultraviolet fluorescence.⁹ This compound was reported by Kestigian *et al.*⁴ to have a hexagonal unit cell ($a_H = 7.288$, $c_H = 27.44$) with nine formula units. According to the same authors¹⁰ this compound is not related to the perovskite structure. According to Seifert and Koknat¹¹ the arrangement of the ions in this unit cell (after Andersen^{11,12}) is based on the AX_6 octahedra which build the perovskite-related compounds of formula ABX_3 . This unit cell with the nine Mn^{+2} ions is shown in Fig. 1. McMurdie *et al.*¹³ propose for CsMnCl_3 the space group $D_{6h}^4-P6_3/mmc$. This space group is inconsistent with Refs. 11 and 12. Rinneberg and Hartman⁶ conclude from NMR measurements that this compound has trigonal symmetry with the space group $D_{3d}^5-R\bar{3}m$, which is consistent with Refs. 11 and 12.

Magnetic measurements were carried out on CsMnCl_3 by Asmussen³ and by Kedzie *et al.*^{7,8} Asmussen³ reported an effective magnetic moment of $6.13\mu_B$ and a Curie-Weiss temperature of -145 °K. Kedzie *et al.*⁷ reported the results of AFMR observations on CsMnCl_3 ; they reported it to be an antiferromagnet with a Néel temperature of (69 ± 3) °K. In another paper⁸ they report that the spins of the Mn^{+2} ions lie in the plane normal to the hexagonal c axis.

We report here the results of a neutron diffraction study of powder sample of CsMnCl_3 . Our results concerning the crystallographic and magnetic structures are in agreement with the results reported in Refs. 4-8, 11, and 12 but inconsistent with 10 and 13.

EXPERIMENTAL

The material CsMnCl_3 was prepared according to the following procedure: Stoichiometric amounts of anhydrous MnCl_2 and CsCl were mixed in a quartz ampoule. The ampoule, after being evacuated and sealed, was heated up to 700 °C and kept at this temperature for several hours, and then slowly cooled down to room temperature. The manganese ion content in the resulting red compound was determined by ethylene diamine-tetraacetic-acid (EDTA) complexometric titration. The chlorine ion content was determined by argentometric titration. Results of the chemical analysis were: Mn, 18.6; Cl, 36.2 (calculated: Mn, 18.67; Cl, 36.15). X-ray measurements were done on a powder sample and a single crystal of CsMnCl_3 and showed it to possess rhombohedral symmetry.⁵

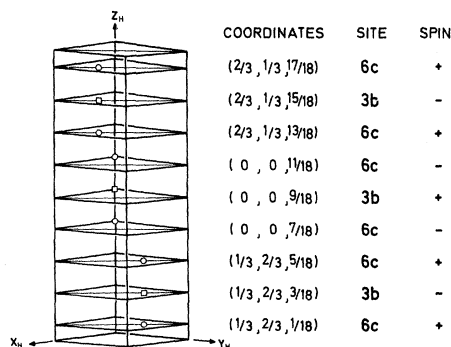


FIG. 1. Crystallographic unit cell with the coordinates, site label (Ref. 14), and relative spin direction of the magnetic ions in CsMnCl_3 . (The ideal close-packing parameter is assumed here for the magnetic ions.)